GLASS MELTING AND ITS INNOVATION POTENTIALS: THE ROLE OF GLASS FLOW IN THE BUBBLE-REMOVAL PROCESS

LUBOMÍR NĚMEC, PETRA CINCIBUSOVÁ

Laboratory of Inorganic Materials
Joint Workplace of the Institute of Inorganic Chemistry AS CR, v.v.i. and the Institute of Chemical Technology Prague, Technická 5, 166 28 Prague, Czech Republic

E-mail: Lubomir.Nemec@vscht.cz

Submitted June 6, 2008; accepted September 19, 2008

Keywords: Bubble removal, Temperature gradients, Glass-flow patterns, Space utilisation, Horizontal channel

This work demonstrates how the temperature distribution and glass-melt flow patterns resulting from these temperature gradients in a simple melting space or tank (horizontal orthogonal channel) influence the bubble removal from the melt, depending on changes of the utilisation (by changes in temperature distribution) of the space for the bubble removal process. The results indicate that the effect of the glass-melt flow pattern and the consequent space utilisation on bubble-removal (fining) may be described by two quantities, namely the virtual height of the bubble rising (the height which the bubble has to rise against downward glass-melt flow to the glass level) and the virtual fraction of dead space for the bubble-removal process (the space ineffective for the removal of the critical bubble). The volume performance of the space for bubble removal [m3s-1] is calculated in this work by using the laboratory values of bubble growth rates (applied to calculate the bubble fining times), the mean residence time of glass in the space and the mentioned two quantities characterizing the space utilisation. The results are intended to support the control regime for optimizing glass-melt flow and developing new concepts of industrial fining spaces designs.

INTRODUCTION

In reaction to the modern problems concerning energy consumption, glass quality and environmental pollution, glass manufacturers have begun to show interest in new glass-melting methods, which are expected to ameliorate or even eventually eliminate the above-mentioned problems. In the search for favourable glass-melting procedures, the nature of the process and its needs should be considered. Glass melting may be characterised as a complex process which is further divisible into the heating, (batch grain (e.g. sand and cords) dissolution and bubble-removal (fining) processes. The requirements of the entire process, namely heat, time and space, predetermine the two significant criteria of the glass-melting process, namely its specific energy consumption and melting performance, as is schematically depicted by Figure 1, which are influenced by the following general factors: temperature, the rate of the homogenisation processes, (here the bubble removal process) the utilisation of the melting space and the heat flux through the outer boundaries [1, 2].

If the specific energy consumption and the volume melting performance upon the condition that no inhomogeneities leave the space with the glass-melt are defined for a simple isothermal melting space without energy recirculation [1], the following two equations are obtained

$$H_M^0 = H_M^T + \frac{\dot{H}^L \tau_H}{\rho V} \frac{1}{u} \tag{1}$$

$$\dot{V} = \frac{V}{\tau_G} = \frac{V}{\tau_H} u \tag{2a,b}$$

where H_M^0 is the specific energy consumption in J/kg; H_M^T is the specific theoretical heat necessary for the chemical reactions, phase transitions and heating of both batch and melt to the melting temperature T to occur (in J/kg); $\dot{H}^L$ is the total heat flux across the space boundary in J/s; τ_H is the reference homogeneization time (here the minimum required bubble removal time upon the condition that bubbles are removed from the quiescent glass layer or the channel with plug flow having the height h_0, see later) in s ; ρ is the glass density in kg/m^3; V - space volume in m^3, $\dot{V}$ - vol. flow rate of melt through the space upon the condition that all inhomogeneities are removed (here the volume fining performance) in m^3/s, $\tau_G = V/\dot{V}$ is the mean residence time of glass in the space and u is the dimensionless quantity designating utilisation of the space for the given process, for which it holds that $u \in \langle 0;1 \rangle$ (see below for the definition of quantity u).

Paper presented at the seminar "Advanced Glass Materials and Innovative Glass Melting Technology in the Year 2020", Brig, Switzerland, March 26-29, 2008.

The calculation of both parameters H^0_M and $\dot{V}$ for the case of the model TV panel glass, using the experimental values of the bubble-growth rates and the dimensions of the model melting space (the horizontal channel, a length of 1m, a width of 0.5 m, a height of the glass layer of 0.5 m, the walls are defined in [1]) using Equations (1) and (2) and under isothermal conditions given in [1] can present the role of the space utilisation in the given region of its validity between 0 and 1. Figures 2a and b present the calculated values for both criteria of the bubble-removal process ($\tau_H = \tau_F$). Figure 2a shows the hyperbolical decrease in the specific energy consumption and Figure 2b the linear increase in the volume fining performance with increasing space utilisation, u. The values of τ_F are calculated based on the Stokes equation using the experimentally measured values of bubble-growth rates. As is apparent from Figure 2a, cases with the space utilisation greater than about 0.5 exhibit only small differences of the specific energy consumption. However, distinct differences may be expected in values of the fining performance - particularly at higher temperatures - because of the linear dependence between the fining performance and space utilisation. The question arises of how the concrete values of the space utilisation, calculated for various bubble histories at different flow structures, influence particularly the values of the fining performance.

The significant role of the space utilisation in melting processes in glass furnaces is well known, and this quantity is usually interpreted in terms of the fraction of dead space and the spectrum of melt-residence times in the melting furnace [3]. The high fraction of dead space arises from the circulation regions and regions with lazy flow. The broad spectrum of melt-residence times in the space is caused by the complex glass flow in the space and results in large quality differences of single homogenisation trajectories. Beerkens declares [4] that the minimum residence time is typically only 15 to 20 % of the average residence time. By other words, not only the rate of homogenisation processes, but also the spacial distribution of inhomogeneities plays an important role in performance of the melting process.

While the character of space utilisation is relatively well comprehensible for processes taking part along melt pathways (the dissolution of sand, chemical homogenisation), the understanding of the same quantity for the bubble-removal process is much less clear. No simple relation exists here between the bubble distribution in the real melting space and the space utilisation for the bubble removal process as results from the mathematical modeling of bubble concentration fields in the glass melting furnace [5,6]. In [8], bubble distributions in a horizontal and vertical fining channel with plug flow demonstrate the maximum space utilisation for a simple continuous space. The spaces without circulation patterns are generally considered most advantageous and spaces with shallow fining bath - either horizontal [9] or vertical [10] - are proposed for the process to avoid circulations. Barton [11], on the contrary, men-

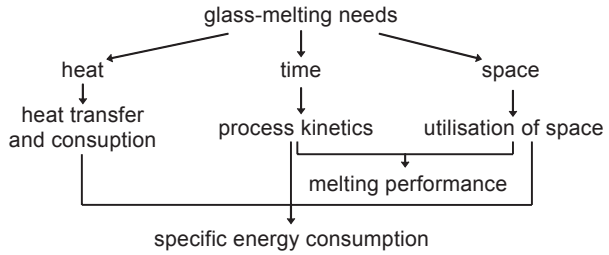

Figure 1. The scheme of the needs of the glass melting process and resulting melting criteria.

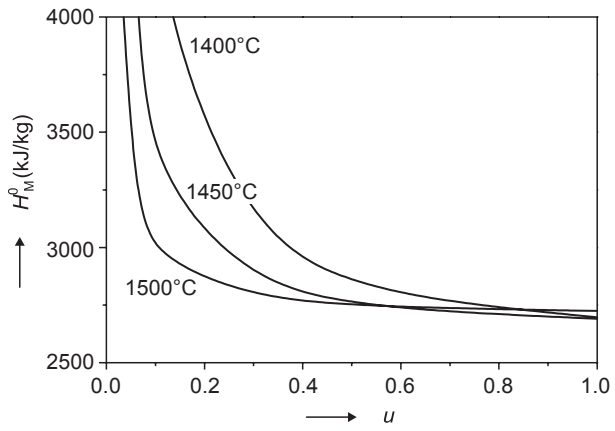

Figure 2a. The dependence between the specific energy consumption of the bubble-removal process, H^0_M and the space utilisation, u, of the horizontal fining channel. Model TV panel glass.

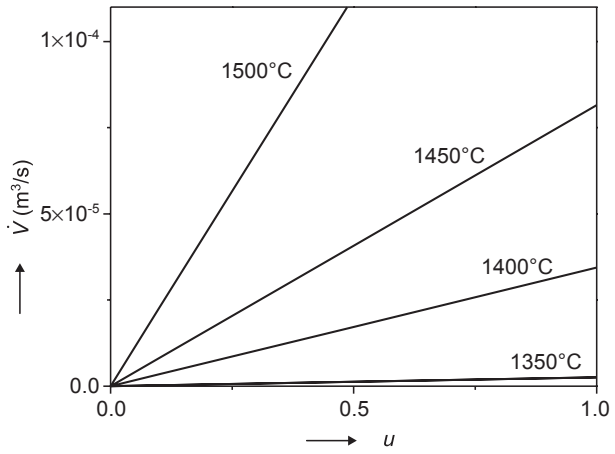

Figure 2b. The dependence between the fining performance, $\dot{V}$, and the value of the space utilisation, u, of the horizontal fining channel. Model TV panel glass.

tions patents utilizing the convective currents to raise the molten glass to the surface and aid fining [12-15] which are characterized by circulations. Consequently, there is no clear evidence which spaces and which flow patterns should exhibit a high fining performance .

The aim of this work is to define and calculate the quantity referred to as 'utilisation of the fining space for the bubble-removal process' in the horizontal continual channel and to study the effect of the glass melt flow pattern caused by temperature dependences on the fining performance of the space.

THEORETICAL

The homogenisation processes (sand dissolution, bubble removal, e.g.) in continuous melting spaces could be classified into two groups:

- homogenisation processes taking place along the melt streamlines
- homogenisation processes with time-temperature histories different from the history along the melt streamlines (bubble removal or settling, e.g.)

The first group comprises such processes as sand dissolution in most commercial glass melting processes as well as chemical homogenisation of the melt, whereas the second group includes the bubble-removal process or particle settling. This work focuses on the bubble-removal process in a horizontal continual channel. The volume fining performance of the channel is defined by Equation (2). For the evaluation of the significance of the space utilisation for the bubble-removal process, two component quantities or parameters have been introduced. The first parameter describes the rate at which the critical bubble moves towards the channel output (the critical bubble attains the glass level just at the end of the channel) with respect to the rate of glass melt in the channel with plug flow and at the same value of $\dot{V}$

$$K^{\mathrm{m}} = \frac{\tau_{\mathrm{G}}}{\tau_{\mathrm{Fcrit}}}; \qquad K^{\mathrm{m}} \geq 1; \tag{3}$$

where τ_{Fcrit} is the residence time of the critical bubble in the channel for the given case.

The value of the virtual fraction of dead space may be defined by

$$m_{\mathrm{virt}} = \frac{\tau_{\mathrm{G}} - \tau_{\mathrm{Fcrit}}}{\tau_{\mathrm{G}}}; \qquad m_{\mathrm{virt}} \in \langle 0;1 \rangle \tag{4}$$

The value of m_{virt} almost merges with the fraction of dead space for glass flow in the case of the horizontal channel, characterized by the longitudinal glass circulation and forward flow near the glass level. In this case, the circulation area theoretically exhibits no glass exchange with the glass through-flow and contains no bubbles. The circulation space is thus the "dead space" for both the glass flow and bubble removal. If other glass pattern is generated in the space, bubbles may be distributed in both the through-flow of glass and in glass circulation areas. The quantity m_{virt} has then no direct geometrical interpretation but nevertheless describes the utilisation of the space from the point of view of bubble forward movement.

On the basis of Equations (3) and (4), Equation (2a) may be expressed as

$$\dot{V} = \frac{V}{K^{\mathrm{m}}\tau_{\mathrm{Fcrit}}} = \frac{V\left(1-m_{\mathrm{virt}}\right)}{\tau_{\mathrm{Fcrit}}} \tag{5}$$

The second introduced parameter involves the height, which the critical bubble should effectively rise relative to the melt in order to reach the glass level. In terms of residence times, this may be expressed as follows

$$K^{\mathrm{Q}} = \frac{\tau_{\mathrm{Fcrit}}}{\tau_{\mathrm{Fplug}}} \tag{6}$$

where τ_{Fplug} is the residence time (rising time) which the critical bubble needs in order to pass through the height of the glass layer, h_0, by free rising. The value of τ_{Fplug} in a quiescent melt or in the channel with plug flow for very small bubbles is roughly proportional to the cube of its fining time

$$h_0 = \frac{2g\rho\dot{a}^2}{27\eta}\tau_{\mathrm{Fplug}}^3 \tag{7}$$

where $\dot{a}$ is the constant bubble-growth rate and η is glass viscosity. If the circulation flows are generated in the channel, the bubble-rising height with respect to the melt becomes dependent on the times that the bubble spends in downward or upward flows. The virtual bubble-rising distance is then given in analogy to Equation (7)

$$h_{\mathrm{virt}} = \frac{2g\rho\dot{a}^2}{27\eta}\tau_{\mathrm{Fcrit}}^3 \tag{8}$$

Proceeding from Equations (6-8), we have

$$K^{\mathrm{Q}} = \frac{\tau_{\mathrm{Fcrit}}}{\tau_{\mathrm{Fplug}}} = \left(\frac{h_{\mathrm{virt}}}{h_0}\right)^{1/3} \tag{9}$$

and if Equations (5) and (9) are combined, the volume-fining performance of the channel may be written as

$$\dot{V} = \frac{V}{K^{\mathrm{m}}K^{\mathrm{Q}}\tau_{\mathrm{Fplug}}} = \frac{V\left(1-m_{\mathrm{virt}}\right)}{\left(\frac{h_{\mathrm{virt}}}{h_0}\right)^{1/3}\tau_{\mathrm{Fplug}}} \tag{10}$$

By comparing Equation (2b) with (10), where u is defined by $1/K^{m}K^{Q}$, the value of τ_H in Equation (2b) is thus given by τ_{Fplug}, i.e. the fining performance is

related to the standard situation of the channel with plug flow. The different temperature distributions in examined cases with different flow patterns influence the bubble fining times and consequently, the values characterizing the utilisation of the space. In order to minimize the impact of temperature regimes of bubble removal on their fining times, the almost constant overall temperature had to be attained in all examined cases of this work.

CALCULATION CONDITIONS AND RESULTS

The mentioned horizontal channel having a length l_0 = 1 m, width w_0 = 0.5 m and height of the glass layer h_0 = 0.5 m was selected as the model space. The glass melt enters the channel in the YZ front plane and exits the channel through the YZ back side. As the model glass, the glass for the production of TV panels was applied. The glass was well characterised, fining property data derived for this glass composition. The temperature dependence of glass density and viscosity is described by the following equations [2]

$$\rho = 2725.1 - 0.238t \; ; \quad (kg/m^3) \quad [t\ (°C)]$$
$$\eta = (2.758\times10^{-2} - 2.410\times10^{-6}t)\exp[6144.6/(t - 437.6)]; \ (Pas)$$

Various melt flow structures were formed by applying appropriate temperature boundary conditions (linear temperature gradients). The following temperature boundary conditions have been applied: a constant temperature over the channel (isothermal channel), horizontal longitudinal temperature gradients with higher temperatures at the channel input or output, horizontal transversal temperature gradients (the gradients across the channel) and mixed horizontal temperature gradients (both longitudinal and transversal temperature gradients).

The experimentally measured dependence of the bubble-growth rate on temperature in K, approximated by the following exponential equation, was used for the computations [16]

$$\dot{a} = \exp[18.969 - 58554/(t + 273.15)] \quad (m/s);$$
$$t\ (°C) \in \langle 1350; 1550 \rangle.$$

The average glass-melt temperature was maintained at approximately 1450°C, the proper fining temperature for this type of glass. The numerical CFD based Glass Furnace Model [17] was applied to calculate the temperature and velocity distributions as well as the bubble trajectories in the horizontal channel (The original form in [17]). A thousand bubbles of the critical radius 5×10^{-5} m (the smallest assumed bubbles) were subsequently put across the entry profile YZ and traced through the channel. The pull out of the channel was then being adjusted until the bubble on the critical trajectory left the melt just at the end of the channel. The resulting pull out and the residence times of the bubbles from entrance till their escape from the melt, involving the critical one, were obtained.

Figures 3, 4 and 5 show the horizontal and vertical longitudinal projections of the selected melt and bubble trajectories in the channels with longitudinal, reversed longitudinal and transversal temperature gradients of 25°C/m. The utilisation of the bubble-removal space in the case of a channel with longitudinal temperature gradient and higher temperature at the input (Figure 3) is obviously low, as bubbles are absent in the circulation flow (see Figure 3b). The longitudinal temperature gradient with a higher temperature at the channel exit (Figure 4) gives rise to longitudinal glass circulation

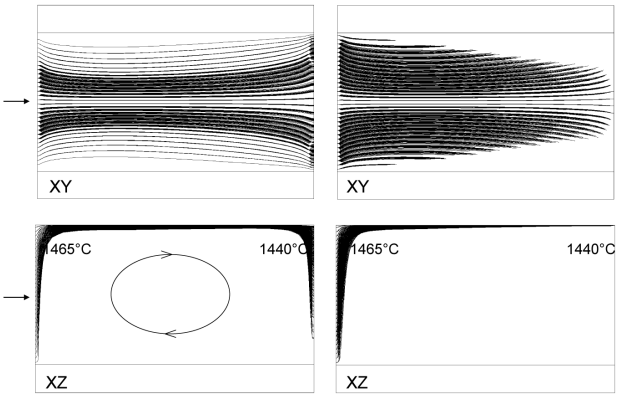

a) b)

Figure 3. The projections of massless-particle and bubble trajectories and in the plane XZ in the horizontal channel with a longitudinal temperature gradient of 25°C/m and a higher input temperature. a) massless-particle trajectories, b) bubble trajectories.

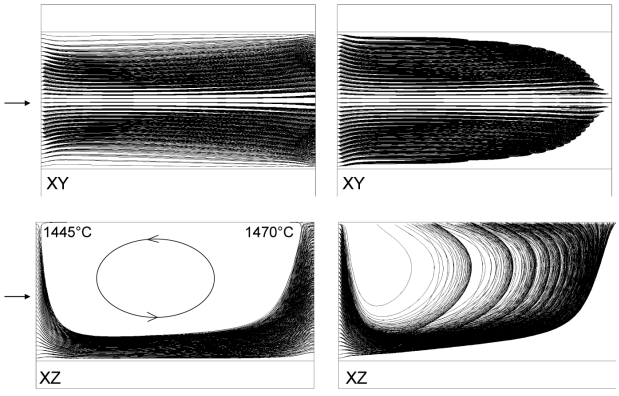

a) b)

Figure 4. The projections of massless-particle and bubble trajectories and in the plane XZ in the horizontal channel with a reversed longitudinal temperature gradient (the channel with a higher output temperature) of 25°C/m. a) massless-particle trajectories, b) bubble trajectories.

as well, but with the direction of the sublevel flow being opposite with respect to the main glass flow. The rotation region of the melt is partially utilised for the bubble-removal process. The space utilisation visually appears higher and will be more precisely expressed by the virtual values derived in Equations (2-10), namely m_{virt} and h_{virt}. The trajectories of the bubbles in channels with pure transversal temperature gradients (Figure 5) have a spiral character.

A 3D representation of the dependence between the volume fining performance of the channel with the higher input temperature and the values of temperature gradients is provided in Figure 6, where the longitudinal temperature gradients are plotted on the x-axis and the transversal temperature gradients on the y-axis. When $y = 0$, only a longitudinal temperature gradient is present, whereas when $x = 0$ only a transversal temperature gradient exists. As expected, the maximum fining performance has been attained in the isothermal channel without circulation flows. Figure 7 presents the same results except for the pure longitudinal and transversal temperature gradients, suggesting that particularly the longitudinal temperature gradient decreases the fining performance of the channel.

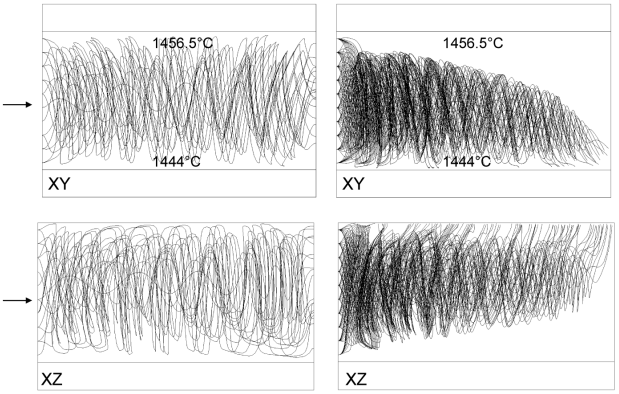

a) b)

Figure 5. The projections of massless-particle and bubble trajectories and in the plane XZ in the horizontal channel with a transversal temperature gradient of 25°C/m. a) massless-particle trajectories, b) bubble trajectories.

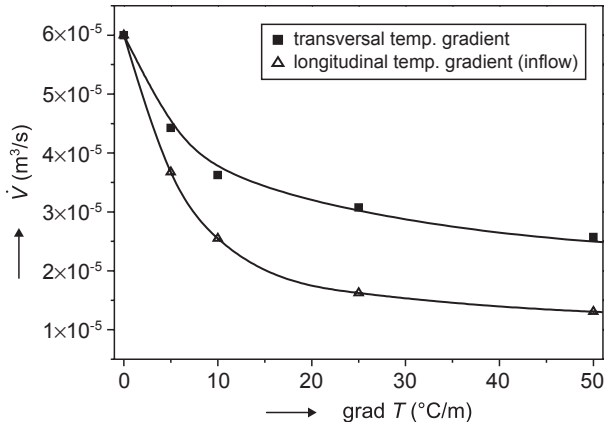

Figure 7. The dependence between the channel fining performance and various types of temperature gradients. The channel with a higher input temperature. △ - the pure longitudinal temperature gradient forming only longitudinal glass flow, ■ - the pure transversal temperature gradient creating only transversal glass flow.

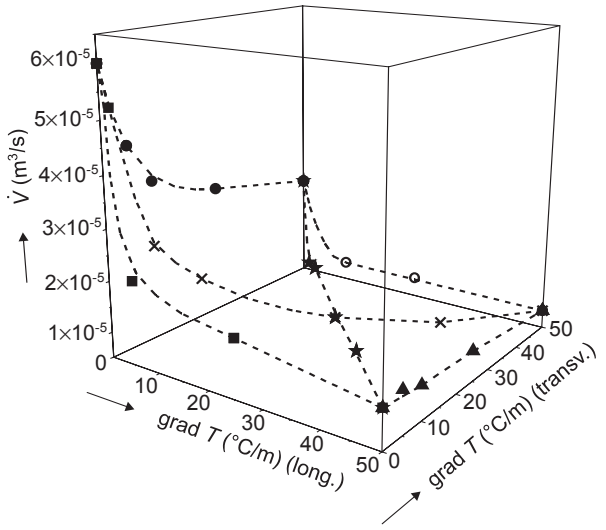

Figure 6. The dependence of the channel fining performance on different types of linear temperature gradients (the applied longitudinal temperature gradient with a higher temperature at the channel input).

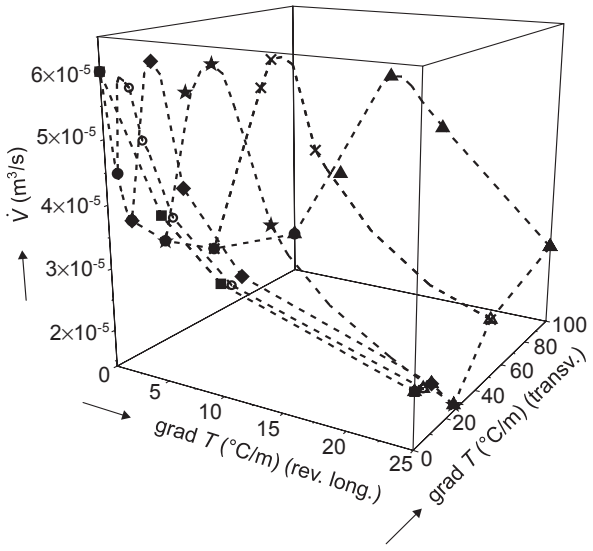

Figure 8. The dependence of the channel fining performance on various types of linear temperature gradients. The channel with a higher output temperature, i.e. the reversed temperature gradient.

The 3D representation of the dependence between the volume fining performance of the channel with the higher output temperature and the values of temperature gradients shows, however, a surprisingly high fining performance for the glass-flow structure caused by the combined temperature gradients, which is characterised by the ratio of the transversal gradient to the longitudinal gradient between 5 and 10 (see Figure 8). Figure 9 shows the relative sharp maxima of the fining performance in the XZ sections (at a constant transversal temperature gradient), with the fining performances being approximately the same as in the isothermal case. The reason for this interesting behaviour may be found by applying the parameters such as the virtual fraction of dead space and the virtual bubble-rising distance (virtual height), characterising the utilisation of the channel space for the bubble-removal process (see Equation (10)).

RESULTS AND DISCUSSION

At a constant temperature, volume and shape of the fining space, the fining performance is directly proportional to the utilisation of the space, as follows from Equation (2b). The resulting value of the space utilisation is ultimately influenced by the ratio between the intensities of the longitudinal and transversal glass flows. The dependences between the values of the virtual dead space, m_{virt}, or the relative virtual height, h_{virt}/h_0, and the values of the pure longitudinal temperature gradient with a higher input temperature (longitudinal glass flow) or the pure transversal temperature gradient (transversal glass flow) are plotted in Figures 10 and 11 (Equations (4) and (9)). Whereas the longitudinal temperature gradient forms a large longitudinal circulation region, as a result of which the high dead space forms in the space and bubbles should rise only through the thin upper layer of the glass forward flow (a low value of h_{virt}, see Figure 3), the transversal temperature gradient creating a transversal circulation of glass is characterised by the very low value of the virtual fraction of dead space and by the high virtual bubble-rising distance, h_{virt}, which the bubble should overcome relative to the melt. The high value of h_{virt} is caused by the fact that the rising bubble spends a longer time in the downward circulating flow than in the upward flow. The fraction of virtual dead space in the case of the pure longitudinal glass melt flow with forward flow near glass level almost merges with circulation area of the melt.

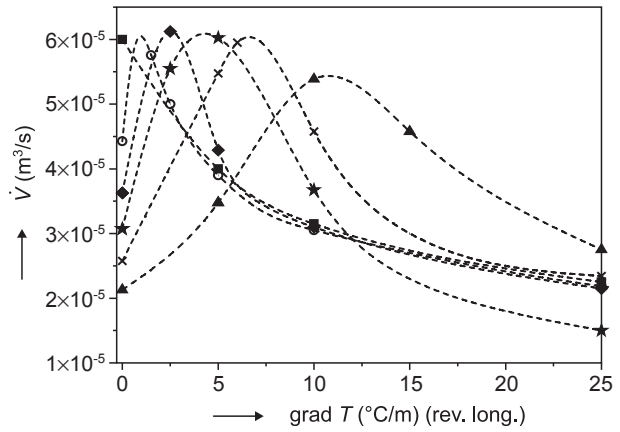

Figure 9. The values of the fining performance as a function of the reversed longitudinal temperature gradient (the gradient with a higher output temperature) in XZ sections (at a constant value of the transversal temperature gradient). Const. transv. temp. grad.: ▲ - 100°C/m, × - 50°C/m, ★ - 25°C/m, ◆ - 10°C/m, ○ - 5°C/m, ■ - 0°C/m.

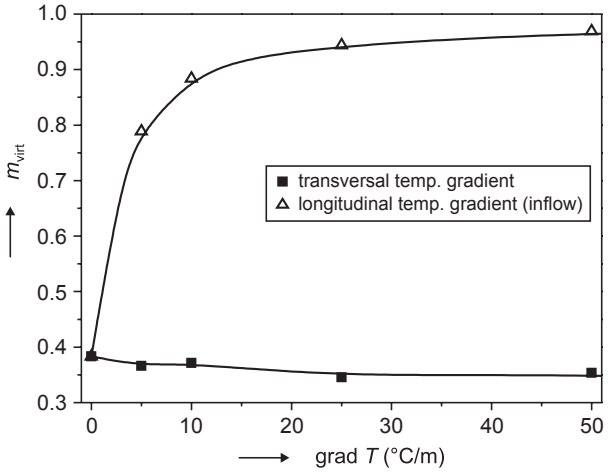

Figure 10. The dependence between the virtual dead space and the value of the pure longitudinal or transversal temperature gradient. The channel with a higher input temperature.

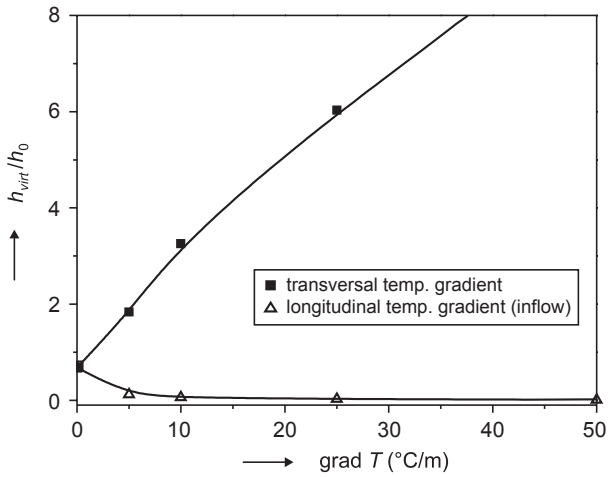

Figure 11. The dependence between the relative virtual height and the value of the pure longitudinal or transversal temperature gradient. The channel with a higher input temperature.

If the circulation flows are considered a part of dead space for glass melt flow, both dead spaces in this case are almost identical. The approximate dependence between the fining performance and fraction of the dead space for melt flow may be described by the Equation [2,18]

$$\dot{V} = \dot{V}_{plug}\left(1-m\right)^{2/3} \tag{11}$$

where $\dot{V}_{plug}$ is the channel fining performance for plug flow and m is the fraction of dead space for glass melt flow.

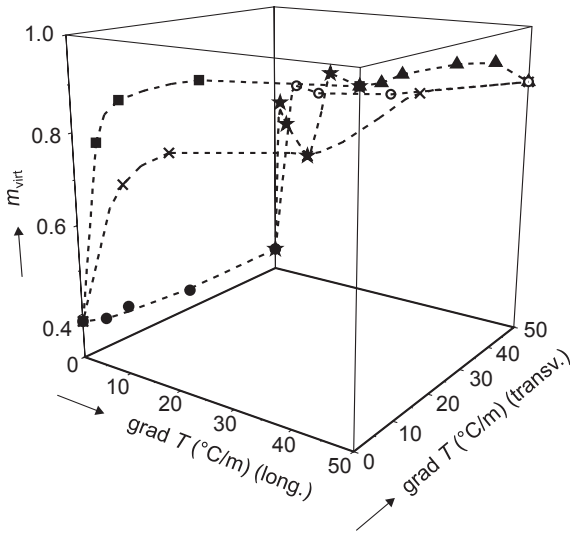

Figure 12. A 3D representation of the virtual dead space as a function of temperature gradients (the channel with a higher input temperature).

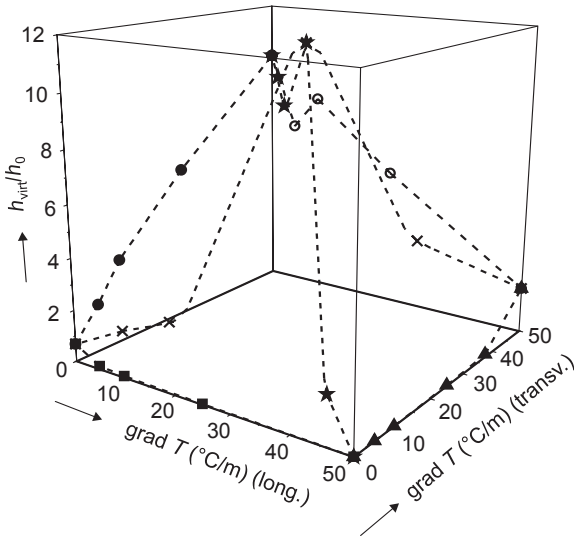

Figure 13. A 3D representation of the relative virtual height as a function of temperature gradients (the channel with a higher input temperature).

The effect of the longitudinal glass melt flow on the value of virtual fraction of dead space generally appears to be very strong and those cases with both longitudinal and transversal glass flows are mostly characterised by a high value of the virtual dead space, by a relatively high virtual bubble-rising distance (virtual height) and consequently, by a low fining performance. This is indicated by the values of the virtual dead space and also by high value of the relative virtual bubble-rising distance (relative virtual height of bubble rising) for the channel with the higher input temperature summarised in the 3D representation in Figures 12 and 13.

In the channel with the pure reversed longitudinal temperature gradient (a higher temperature at the channel exit), critical bubbles move in the lower part of the channel and with a part of their trajectory move also through the circulation area and backward flow (see Figure 4). The virtual dead space is therefore lower and the relative virtual height higher than in the previous case (see Figure 14).

In the channels with mixed temperature gradients, the effects of the longitudinal and transversal glass flows are combined, with the influence of longitudinal flows (triggered by longitudinal temperature gradients) being also for the bubble-removal process less favourable as compared to the transversal flow. The reversed longitudinal gradients provide generally higher fining performances than the gradient with the higher input temperature. The flow structures evoked by combined temperature gradients with the ratio of the transversal to longitudinal gradient of between 5-10 are interesting cases where high fining performance is obtained, namely around the value for the isothermal channel (6×10^{-5} m^3/s) (see Figures 8-9). The analysis of the glass-flow structure by means of m_{virt} and h_{virt}/h_0 has

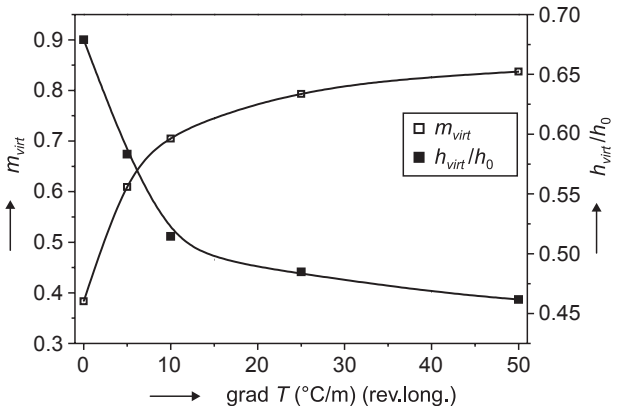

Figure 14. The dependence between the virtual dead space, m_{virt}, as well as the relative virtual height, h_{virt}/h_0, and the pure longitudinal temperature gradient. The channel with a higher output temperature (a reversed temperature gradient). □ - the virtual dead space, m_{virt}, ■ - the relative virtual height, h_{virt}/h_0.

revealed that the mentioned favourable cases are always characterised by a minimum value of m_{virt} and at the same time by a low value of h_{virt}/h_0. This fact is depicted in Figures 15 and 16, which provide the dependences between both the quantities and the longitudinal temperature gradient at various constant transversal temperature gradients (in the XZ sections). In the search for the physical reason for such behaviour, the trajectories of critical bubbles ought to be examined. Figures 17a-c provide the trajectories of the critical bubbles in the XZ projections for the cases characterised by the transversal temperature gradient of 50°C/m and longitudinal temperature gradients of 0, 5 and 10°C/m. In the case of the zero longitudinal gradient, the critical bubble circumscribes the spiral path with a relatively high number of circles (Figure 17a), from which the high value of a h_{virt}/h_0 arises. The fining performance is therefore relatively low. The optimum case in Figure 17b, characterised by the maximum fining performance, exhibits a minimal value of m_{virt}, as the spiral bubble trajectory has slightly shifted to the region of low forward glass velocities and simultaneously shows much lower h_{virt}/h_0 due to the decreased number of bubble circles. At a still higher longitudinal temperature gradient of 10°C/m, as shown in Figure 17c, the large virtual dead space forms in the upper part of the channel and the critical bubble is pulled down to the channel bottom. The steep increase in the value of m_{virt} is not compensated by the decrease in h_{virt}/h_0, and the fining performance decreases rapidly.

CONCLUSION

The utilisation of the melting space for single dissolution or bubble removal processes is one of the crucial factors determining the energy consumption and melting performance of the space. Two parameters defined in this work have been derived in this work, namely the virtual dead space and the virtual bubble-rising distance (the virtual height). Their simple combination has been used to demonstrate the fining behaviour, in a melting space having the form of a horizontal channel, and dependent on temperature gradients. The evident and known optimum case of the fining process is the parallel flow of the melt with bubbles (the plug flow or the flow with the parabolic melt velocity distribution) at isothermal conditions. However, the results of this and previous works have shown that even very small temperature gradients (2°C/m) give rise to the circulation flows which apparently reduce the fining performance of the space [2,18]. At that point, the isothermal fining appeared to be a technical problem. The calculations and analysis results using the virtual dead space and virtual height, however, have also shown that alternative, properly-set temperature boundary conditions may determine the glass flow pattern, which is beneficial for the given process in terms of the space utilisation. The beneficial flow conditions in this work have been characterised by a relatively strong transversal circulation combined with a weak longitudinal circulation having forward flow near the bottom. The mentioned

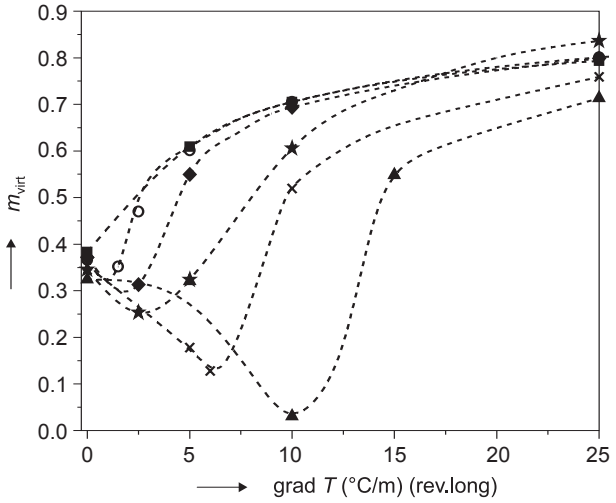

Figure 15. The dependence between the virtual dead space, m_{virt}, and the longitudinal temperature gradient at various constant values of the transversal temperature gradients (in the XZ sections through the channel). The channel with a higher output temperature (a reversed temperature gradient). Const. transv. temp. grad.: ▲ - 100°C/m, × - 50°C/m, ★ - 25°C/m, ◆ - 10°C/m, ○ - 5°C/m, ■ - 0°C/m.

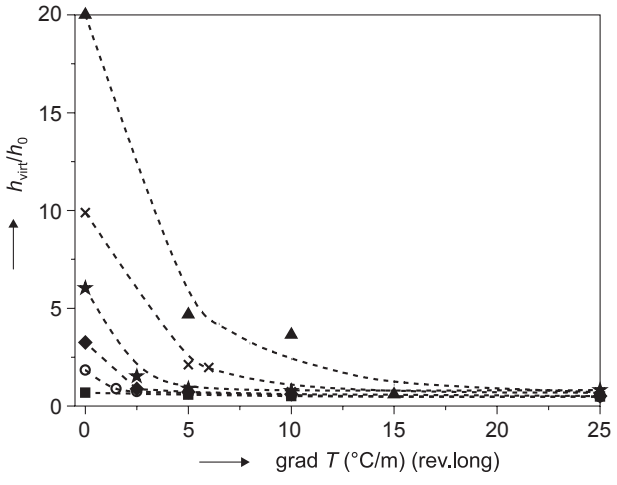

Figure 16. The dependence between the relative virtual height, h_{virt}/h_0, and the longitudinal temperature gradient at different constant values of the transversal temperature gradients (in the XZ sections through the channel). The channel with a higher output temperature (a reversed temperature gradient). Const. transv. temp. grad.: ▲ - 100°C/m, × - 50°C/m, ★ - 25°C/m, ◆ - 10°C/m, ○ - 5°C/m, ■ - 0°C/m.

optimum glass melt flow has been determined by the transversal and longitudinal temperature gradients whose values were in the ratio of 5-10. This combination gives a low value for the virtual dead space and virtual bubble-rising distance (virtual height) for the critical bubble to ascend and thus a high fining performance $\dot{V}$. The values of the channel fining performance were comparable with the isothermal case. It seems that setting the conditions characterising the mentioned favourable region of temperatures and consequently melt flows would be easier than strictly isothermal fining.

The results help to understand the property utilisation of the space and its significance for the fining process. New designs for fining tanks or fining processes may be proposed including the optimum settings of the process parameters (e.g. temperature, temperature gradients, melt mechanical stirring) to achieve optimum fining at lowest possible energy consumption. The fundamental evaluation of the present industrial furnaces by the here defined approaches on space utilisation is partially restricted by the time-temperature histories differing for the melt and consequently also for bubbles, complicating the comparison of different cases. Further calculations are needed to understand better the influence of the bubble-growth rate (which is determined by temperature and glass melt composition) on the optimal glass-flow patterns in terms of fining.

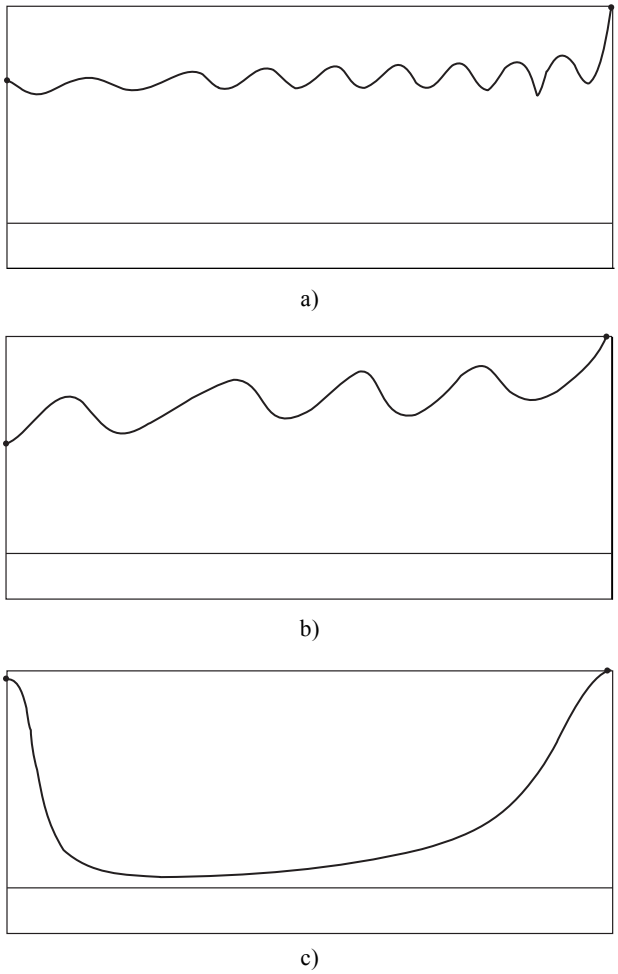

Figure 17. The XZ projections of the trajectory of the critical bubble in the channel with the combined reversed longitudinal temperature gradient (the channel with a higher output temperature) and the transversal temperature gradient; a) the pure transversal temperature gradient of 50°C/m, b) the longitudinal gradient of 5°C/m, the transversal gradient of 50°C/m, c) the longitudinal gradient of 10°C/m, the transversal gradient of 50°C/m.

Acknowledgement

This work is part of Project No. 2A-1TP1/063, "New glass and ceramic materials and advanced concepts of their preparation and manufacturing", implemented with the financial support of the Ministry of Industry and Trade and the Institutional Research plan Proposal No. Z40320502 "Design, synthesis and characterisation of clusters, composites, complexes and other compounds based on inorganic substances; mechanisms and kinetics of their interactions".

References

1. Němec L., Jebavá M.: Eur. J. Glass Sci. Technol. A 47, 68 (2006).
2. Němec L., Jebavá M., Cincibusová P.: Ceramics-Silikáty *50*, 140 (2006).
3. Simonis F., de Waal H., Beerkens R.: Collected Papers XIV. International Congress on Glass, Vol. III, pp. 118-127, New Delhi, India 1986.
4. Beerkens R.: Ceramics-Silikáty *52*, 206 (2008).
5. Balkanli B., Ungan A.: Glass Technol. *37*, 164 (1996).
6. Matyáš J., Němec L.: Glastechn. Ber. Glass Sci. Technol. *76*, 71 (2003).
7. Kloužek J., Němec L., Jebavá M., Trochta M., Brada J.: Ceramics-Silikáty *51*, 225 (2007).
8. Cincibusová P., Němec L.: Ceramics-Silikáty *49*, 286 (2005).
9. Plumat E.: Glass Ind. *54*, 22 (1973).
10. Anon E.: Glass Ind. *69*, 19 (1988).
11. Barton J. L.: Collected Papers XVI International Congress on Glass, Vol. 1, pp.165-184, Madrid, Spain 1992.
12. Noiret R. et al.: French Patent 2 550 523 (19.08.83).
13. Martlew D.: European Patent 0 403 183 (13.06.89).
14. Trevelyan R. E.: European Patent 0 403 184 (13.06.89).
15. Cozac D. et al.: US Patent 5 078 777 (29.04.88).
16. Unpublished results.
17. Schill P.: Proceedings of the 2nd International Seminar on Mathematical Simulation in the Glass Melting, pp. 102-116, Vsetín-Horní Bečva, Czech Republic, May 17-19, 1993.
18. Cincibusová P., Němec L., Jebavá M.: Proceedings of the 9th International Seminar on Mathematical Modeling of Furnace Design and Operation, pp. 33-42, Velké Karlovice, Czech Republic, June 2007.

TAVENÍ SKEL A JEHO INOVAČNÍ POTENCIÁL: ÚLOHA POVAHY PROUDĚNÍ V TAVICÍM PROSTORU PŘI ODSTRAŇOVÁNÍ BUBLIN.

LUBOMÍR NĚMEC, PETRA CINCIBUSOVÁ

Laboratoř anorganických materiálů,
Společné pracoviště Ústavu anorganické chemie AVČR, v.v.i.
a Vysoké školy chemicko-technologické v Praze,
Technická 5, 166 28 Praha

Práce ukazuje význam struktury proudění v modelovém tavicím prostoru tvaru pravoúhlého otevřeného kanálu, vyvolané teplotními gradienty v roztaveném skle, na průběh odstraňování bublin. Je zavedena veličina využití tavicího prostoru, kterou lze zjistit modelováním chování bublin v daném prostoru. Veličinu využití tavicího prostoru lze definovat pomocí dvou parciálních veličin, virtuálního mrtvého prostoru pro odstraňování bublin a virtuální výšky, kterou musí kritická bublina překonat vůči okolní tavenině při svém vzestupu k hladině. Modelováním byly vypočteny obě parciální veličiny a maximální výkony modelovaného tavicího prostoru s využitím laboratorně získaných hodnot rychlosti růstu bublin. Byla nalezena struktura proudění, která je pro daný prostor a děj velmi výhodná. Využití výsledků se předpokládá pro porovnávání využití tavicích prostorů existujících tavicích zařízení a pro návrhy nových prostorů.